

First-principles calculations of boron-related defects in SiO₂

Minoru Otani,* Kenji Shiraishi, and Atsushi Oshiyama

Institute of Physics, University of Tsukuba, Tennodai, Tsukuba 305-8571, Japan

(Received 20 August 2003; published 21 November 2003)

We report first-principle total-energy calculations that provide stable and metastable geometries and diffusion mechanisms of boron in SiO₂ with point defects which contain O vacancies and O interstitials. We find that a B atom forms various stable and metastable geometries in SiO₂ with point defects, depending on its charge state and surrounding environments. We also perform calculations that clarify the chemical feasibility of bonding configurations between a B atom and constituent atoms in SiO₂. It is found that wave function distribution around the impurity and its occupation are essential to determine the geometry for each charge state. Binding energies of a B atom with constituent atoms in SiO₂ are decisive factors to the bond configuration around the B atom. In the case of B in SiO₂ with an O interstitial, a B atom forms a very stable B-O complex in which the B atom is bound to the O interstitial. Once the B-O complex is formed, the B atom diffuses via the SiO₂ network keeping this B-O unit with unexpectedly small activation energies of 2.1–2.3 eV. The calculated activation energies agree well with the data experimentally available.

DOI: 10.1103/PhysRevB.68.184112

PACS number(s): 66.30.Jt, 81.65.Mq, 71.15.Nc, 71.55.–i

I. INTRODUCTION

Atomic diffusion in materials is one of the fundamental phenomena.^{1,2} Particularly in the semiconductor industry, dopant diffusion in semiconductors during fabrication processes is essential to realize designed performances of devices. Hence a much of effort has been devoted to clarifying mechanisms of the atomic diffusion in semiconductors, mainly in Si.^{3–8}

Along with the recent trend of miniaturization of metal oxide semiconductor (MOS) devices, ultrathin silicon oxide films are demanded for use as gate oxide films for MOS and other devices. As the thickness of the films is decreased, the problem of impurities, e.g., B atoms diffusing into the SiO₂ film from the gate electrode and further penetrating into the silicon substrate, becomes serious.⁹ Experimentally, it is reported that H, F, and Cl atoms accelerate the penetration of B atoms, while oxinitride films decrease their penetration.^{9–12} A model for B diffusion in SiO₂ is proposed by compiling thermochemical data.¹³ In that model the B atom diffuses in SiO₂ via a peroxy linkage (PL) defect, -Si-O-O-Si-. However, the suppression mechanisms of the B penetration and the diffusion mechanisms of B atoms in SiO₂ have not been clarified yet. Theoretically Fowler *et al.* investigated B diffusion models using semiempirical quantum chemical calculations and proposed a model in which the B atom diffuses by exchanging its position to the Si atom.¹⁴ To increase the reliability of ultrathin gate oxide films, it is essential to clarify both stable geometries of B atoms and atomistic mechanisms of B diffusion in SiO₂. Recently, we have clarified both stable geometries and the diffusion mechanisms of B in defect-free SiO₂ using first-principle total-energy calculations.¹⁵ The results showed that a B atom forms various stable and metastable geometries depending on its charge state. In addition, we have clarified that the B atom diffuses by breaking and forming bond configurations in SiO₂ networks, and that the diffusion mechanism also differs depending on the charge state. The calculated activation energies agree well with those obtained experimentally.¹²

Since actual thermal oxide films have an amorphous structure, they are considered to contain some defects such as O vacancies and O interstitials, which do not conform to the stoichiometry of SiO₂ at local regions. Actually, during the synthesis of silica glasses, the number of O vacancies increases as the oxygen flow is decreased, and the number of O interstitials increases as the oxygen flow is increased.¹⁶ Therefore, to clarify the diffusion mechanisms of B in the oxide film, it is important to elucidate the stable geometries and the diffusion mechanisms of a B atom not only in defect-free SiO₂ but also in SiO₂ with point defects. In this paper, we explore the stable and metastable geometries of a B atom in SiO₂ with point defects in which the O vacancies and the O interstitial exist as defects, using first-principle total-energy calculations. A B atom is bound to these defects forming various chemical bonds. To clarify the chemical feasibility of bonding configurations between the B atom and the constituent atoms in SiO₂, we make a comparative study on the stable and the metastable geometries of the B atom in defect-free SiO₂. We have found that the B atom binds strongly to the O interstitial and forms a threefold coordinated geometry with nearby O atoms. This is because the B-O bond is stronger than the Si-O bond. It has also been found that configurations in which the B atom binds to an O vacancy are metastable geometries in all regions of μ_{Si} due to the weakness of the Si-B bond. Furthermore, we have clarified that the activation energies of the B diffusion in SiO₂ with point defects are comparable to those in defect-free SiO₂, irrespective of the presence of O related defects.

II. CALCULATION

Density-functional theory (DFT) is used within the generalized-gradient approximation (GGA).^{17–19} Norm-conserving pseudopotentials for Si (Ref. 20) and ultrasoft pseudopotentials for O and B (Ref. 21) are adopted to describe the electron-ion interaction. The cutoff energy of the plane-wave basis set is 25 Ry. We use the Γ point for the Brillouin zone (BZ) sampling.²² Geometries are optimized

for all atoms until the remaining force on each atom is less than 5 mRy/Å.

Network former impurities such as B, P, and As, are known to diffuse by reacting with the SiO₂ network. Thus diffusion barriers are likely to be dominated by local bonding effects. Though the actual oxide films have an amorphous structure, it consists of a continuous network of corner-sharing SiO₄ tetrahedra. In this study, we employ a supercell containing 72 atoms in a α quartz as a representative of containing a network of corner-sharing SiO₄ structure. To simulate a B atom diffusion in the oxide films we calculate following two types of defects in the α quartz. In one case, a B atom is bounded with a PL defect (an O interstitial) and in another, a B atom is bound to O vacancies. To obtain the diffusion pathways and activation energies, the energy surface in multidimensional space must be known. We used the constraint-minimization method²³ in this study. This is a method of converting the problem of searching the path in N -dimensional space into a structural optimization problem with a constraint in the $(N-1)$ -dimensional space. Here, N is the degrees of freedom of atoms contained in a unit cell.

The formation energy of a structure with defect α is defined by

$$E_f(\alpha, Q, \mu_e, \mu_\beta) = E_{\text{tot}}(\alpha, Q) - Q\mu_e - \sum_{\beta} n_{\beta}\mu_{\beta},$$

where $E_{\text{tot}}(\alpha, Q)$ is the total energy of the supercell containing the defect α with a charge state Q , μ_e is the electron chemical potential, i.e., Fermi level in the energy gap, n_{β} is the number of β atoms ($\beta = \text{Si}, \text{O}, \text{B}$) in the supercell, and μ_{β} is the chemical potential of a β atom. For the charged state Q , we consider +1 ($Q=1$), neutral ($Q=0$), and -1 ($Q=-1$) charged state. The value of μ_e when $E_f(\alpha, Q, \mu_e, \mu_{\beta}) = E_f(\alpha, Q+1, \mu_e, \mu_{\beta})$ is defined as $\mu_{\text{th}}(Q/Q+1)$. This value is called the thermodynamic level, which determines the stability of the charged states with Q and $(Q+1)$.¹³ The chemical potentials of bulk Si and O₂ molecules are chosen as the maximum values for μ_{Si} and μ_{O} , respectively, and satisfy the relation $\mu_{\text{Si}} + 2\mu_{\text{O}} = \mu_{\text{SiO}_2}$, where μ_{SiO_2} is the total energy per molecule in SiO₂. Under these conditions, the range of values for μ_{Si} is $\mu_{\text{Si(bulk)}} - 2\mu_{\text{O(mol)}} \leq \mu_{\text{Si}} \leq \mu_{\text{Si(bulk)}}$.

For the analysis of the structural deformation of a SiO₄ tetrahedron, we have introduced a tetrahedral distortion parameter t . The tetrahedral distortion is defined by way of the sum of angles of three Si-O-Si bonds. A regular tetrahedron consisting of sp^3 hybridization has a total angle of 328.5°, whereas a planar trigonal structure consisting of sp^2 hybridization has the total angle 360°. We define the tetrahedral distortion as one when the total angle corresponds to the sp^3 hybridization, and we define it as zero when that corresponds to the sp^2 hybridization. The tetrahedral distortion is then defined as $t = (360 - \sum_{l=1,3}\alpha_l)/31.5$, where α_l is an angle of Si-O-Si bond.

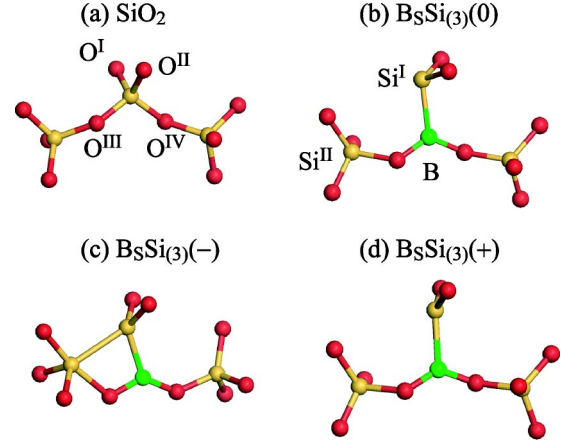


FIG. 1. (Color online) Geometric structures of total-energy minimized (a) α quartz, (b) B_SSi₍₃₎(0) [Fig. 1(a) in Ref. 15], (c) B_SSi₍₃₎(-), and (d) B_SSi₍₃₎(+). Signs + and -, and 0 in parentheses denote the +1 charged state, the -1 charged state, and the neutral state, respectively. Only a part of the atoms in a unit cell are shown to avoid visual complexity.

III. STABLE GEOMETRIES OF B ATOM IN SiO₂

A. B atom in defect-free SiO₂

Figure 1 shows a part of atomic geometries of SiO₂ and B_SSi₍₃₎ for each charge state. As shown in Fig. 1(a), the atomic geometry of SiO₂ is continuation of corner-sharing SiO₄ tetrahedra, with twofold coordinated O atoms in the Si-O-Si bridge form. In the neutral charge (0) state, B_SSi₍₃₎(0) [Fig. 1(b)] is the most stable geometry [Fig. 1(a) in Ref. 15]. A B atom is threefold coordinated with Si and two O atoms, whereas the bond configurations of Si^I are changed from fourfold to threefold coordinated. We have found that the B_SSi₍₃₎(0) has a localized state originated from a silicon dangling bond in the gap. To clarify the spatial distribution of the localized state, we have shown isosurfaces of the wave functions in Fig. 2. As seen from Fig. 2(a), the wave function of the highest occupied state is localized on the undercoordinated Si^I atom as well as on the B-Si^I bond. An electron is accommodated in the localized state so that the spin is 1/2. In the negatively charged (-1) state, B_OSi₍₅₎ is the most stable geometry [Fig. 1(c) in Ref. 15]. B_SSi₍₃₎(-) [Fig. 1(c)] is a metastable geometry and is higher than B_OSi₍₅₎ in total energy by 0.77 eV. The main structural relaxation of the B_SSi₍₃₎(-) relative to the B_SSi₍₃₎(0) results in the strong tetrahedral distortion on the undercoordinated Si^I atom. To accommodate an additional electron in the half occupied localized state of B_SSi₍₃₎(0), Si^I forms a new bond (so-called floating bond²⁴) with Si^{II} associated with structural deformation. Hence, the Si^{II} atom becomes fivefold coordinated. The wave function of the highest occupied state is thus distributed mainly on the Si^I-Si^{II} floating bond and on the B-Si^I bond around the B atom [Fig. 2(b)]. In the positively charged (+1) state, B_{Ox}O₍₃₎ is the most stable geometry [Fig. 1(e) in Ref. 15]. When an electron is removed from B_SSi₍₃₎(0), a positively charged state B_SSi₍₃₎(+) [Fig. 1(d)] is obtained, which is found to be a metastable geometry of which energy is 0.50 eV higher than the B_{Ox}O₍₃₎ geometry.

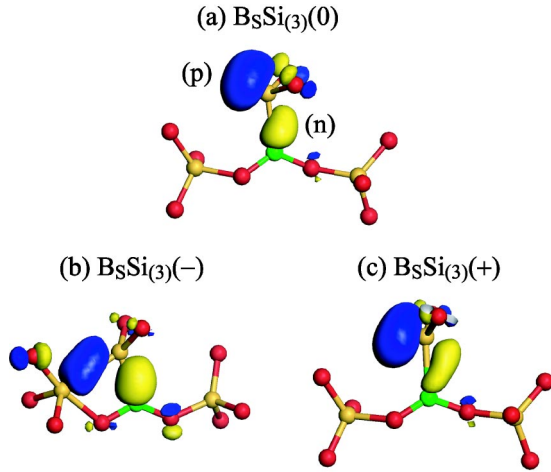


FIG. 2. (Color online) Wave functions at the Γ point of (a) the highest occupied state of $B_5Si_3(0)$, (b) the highest occupied state of $B_5Si_3(-)$, and (c) the lowest unoccupied state of $B_5Si_3(+)$. Blue (p) and yellow (n) isosurfaces denote the positive and negative values of the wave function, respectively.

In $+1$ charged state the localized state of $B_5Si_3(0)$ [Fig. 2(a)] is empty. The planar sp^2 -like bonding configuration is clearly shown in Fig. 1(d). The spatial distribution of the wave function of the lowest unoccupied state is shown in Fig. 2(c). Due to the lack of an electron, it is clear that a p component in the wave function of the localized unoccupied state is a little larger than that in neutral charge state. Thus Si^I atom forms the sp^2 hybridized configuration in $+1$ charged state.

The bond length and the distortion of the tetrahedron t for B_5Si_3 geometry are listed and compared for various charge states in Table I. We have also shown the bond length and t for SiO_2 as a reference. The distance between Si^I and Si^{II} atoms drastically increases as an electron is removed from the localized state as described in Table I, namely, the floating bond is stable only for the negatively charged state. The decrease in occupation number of the defect state also causes slight B- Si^I bond elongation. This can be understood as fol-

TABLE I. Interatomic distances (\AA) and tetrahedral distortion parameter t (see text) of the geometries in Fig. 1. The name of atoms with/without Greek superscript in the first column correspond to the symbols of the atoms in Fig. 1.

	SiO_2	$B_5Si_3(-)$	$B_5Si_3(0)$	$B_5Si_3(+)$
Si^I-Si^{II}	3.092	2.427	3.472	3.641
Si^I-O^I	1.617	1.672	1.649	1.579
Si^I-O^{II}	1.617	1.641	1.662	1.581
Si^I-O^{III}	1.622	2.554	2.883	2.899
Si^I-O^{IV}	1.622	3.038	2.918	2.804
$Si^{II}-O^{III}$	1.617	1.941	1.636	1.647
B- Si^I		1.929	1.984	1.991
B- O^{III}		1.358	1.360	1.340
B- O^{IV}		1.383	1.358	1.348
$t(Si^I)$	1.005	0.882	1.282	0.209

lows. In the -1 charged state, the wave function shown in Fig. 2(b) has a large amplitude between the B and Si^I bond, then the B- Si^I bond is considerably strengthened by the distribution of the wave function. In the neutral state, on the other hand, the amplitude is rather smaller to some extent, so that the B- Si^I bond length is slightly longer than that in the negatively charged state. In the $+1$ charged state, since an electron is removed from the localized state [Fig. 2(c)], the B- Si^I bond strength becomes weaker than that in other charged states. As seen from the bond configuration of Si^I in Fig. 1, the tetrahedral distortion may be different for each charge state. Though Si^I is fourfold coordinated in the -1 charged state, the tetrahedral distortion is slightly smaller than 1. This is indicative of forming the floating bond with Si^{II} atom associated with structural deformation. In the neutral state, the tetrahedral distortion is slightly larger than 1, which is typical for the dangling bond on undercoordinated silicon atom. Due to the absence of an electron in the localized state in the $+1$ charged state, the bonding configuration of Si^I is stabilized by forming sp^2 -like bond configuration. Hence the tetrahedral distortion of the $+1$ charged state decreases close to zero.

B. B atom with O vacancies

We have found that a B atom takes a variety of stable and metastable geometries depending on its charge state in defect-free SiO_2 .¹⁵ Yet the thermal oxidized SiO_2 films might have various defects, we further elucidate the stable and metastable geometries of a B atom which is binding with the various defects in SiO_2 . Here, we clarify the stable and metastable geometries of the B atom in SiO_2 containing O vacancies in the neutral state ($Q=0$). Figure 3 shows a part of the atomic geometries of the O vacancy, and the stable and the metastable geometries for the B atom binding with the O vacancy. First, we have explored the stable geometry including the single O vacancy in SiO_2 in the neutral state and found that the two dangling bonds on Si^I and Si^{II} . It has also been found that a new Si^I-Si^{II} bond is formed with structural deformation as shown in Fig. 3(a). This stable geometry corresponds to that obtained in previous calculations.²⁵⁻²⁹ When a B atom is bound with an O vacancy, the stable geometry is $B_{S(2)}$ [Fig. 3(b)], in which the B atom is substituted into the O vacancy site and forms a twofold coordinated geometry with Si^I and Si^{II} . In $B_{S(2)}$ geometry the Si^{III} atom maintains the Si-O-Si bond with O^I and Si^{IV} . In a metastable geometry, on the other hand, $B_{S(3)}$ [Fig. 3(c)] is obtained. The B atom is substituted into an O vacancy site, as in the case of $B_{S(2)}$, however, it breaks the $Si^{III}-O^I$ bond and forms a threefold coordinated ($Si \equiv B$) geometry with nearby Si atoms. The total energy of $B_{S(3)}$ geometry is higher by 2.11 eV than that of $B_{S(2)}$ due to the higher binding energy of Si-O bond compared to that of the Si-B bond.

Secondly, we have calculated the stable geometries of a B atom in the case where an O^I site shown in Fig. 3(a) is replaced by a vacancy, namely, two O vacancies exist in SiO_2 . The stable geometry $B_{S(3)}O_V$ and the metastable geometry $B_{S(2)}O_V$ are shown in Figs. 3(d) and 3(e), respectively. In $B_{S(2)}O_V$ geometry, the $Si^{III}-B$ bond is broken and

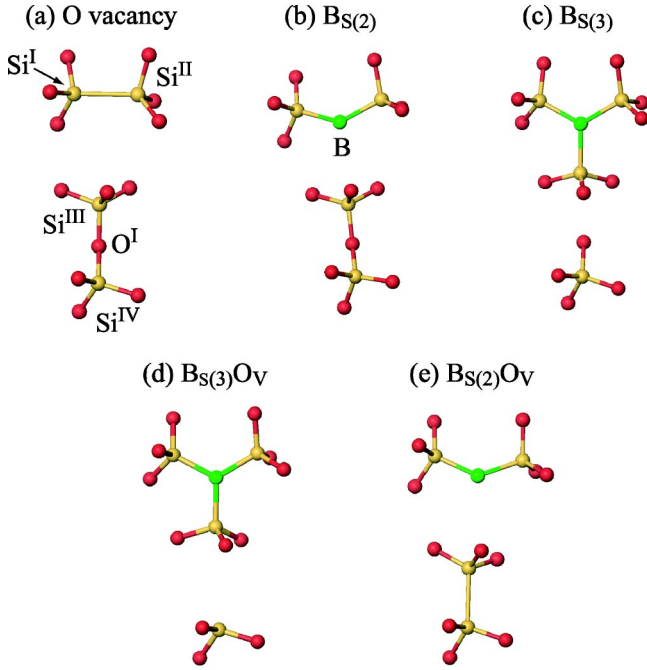


FIG. 3. (Color online) Geometric structures of total-energy minimized (a) an O vacancy, (b) $B_{S(2)}$, (c) $B_{S(3)}$, (d) $B_{S(3)O_V}$, and (e) $B_{S(2)O_V}$. Only a part of the atoms in a unit cell are shown to avoid visual complexity.

Si^{IV} is bound with Si^{III} ; the total energy for $B_{S(2)O_V}$ is higher by 0.66 eV than that of $B_{S(3)O_V}$. Basically a B atom prefers a threefold coordinated geometry to a twofold one. Although both $B_{S(3)}$ and $B_{S(3)O_V}$ geometries have $Si \equiv B$ bonds, $B_{S(3)}$ is a metastable geometry in SiO_2 with a single O vacancy, whereas $B_{S(3)O_V}$ is the most stable geometry in SiO_2 with double O vacancies. This can be understood as follows. In $B_{S(3)}$ geometry the $Si^{III}-O^I$ bond is broken and then a new bond between B and Si^{III} atoms is formed. The Si-O bond, however, is stronger than the Si-B bond in energy by 5.3 eV.³⁰ Consequently, $B_{S(3)}$ geometry becomes metastable due to the energy consuming bond recombination. On the other hand, in the case of the conversion from $B_{S(2)O_V}$ to $B_{S(3)O_V}$, the bond length of $Si^{III}-Si^{IV}$ is 2.48 Å, which is longer than that in bulk Si of 2.37 Å; hence, the $Si^{III}-Si^{IV}$ bond is a weak bond. Thus the bond is easily broken and the energy loss is small. Therefore, $B_{S(3)O_V}$ is the most stable configuration.

C. B atom with an O interstitial

Next, we have performed an extensive search for the stable and the metastable geometries of a B atom with an O interstitial. Among various geometries of the O interstitial, we have found that the PL geometry [see Fig. 4(a)] is the most stable geometry for the neutral charge state. This stable geometry was also found in previous calculations.³¹⁻³⁴ In $B_{(2)O_I}$ [Fig. 4(b)], which is metastable geometry, the B atom intervenes between O^I and O^{II} and is twofold coordinated ($-O^I-B-O^{II}-$). Furthermore, we have found another stable geometry $B_{(3)O_I}$, which is lower than $B_{(2)O_I}$ in total energy by 0.65 eV. The B atom breaks the Si^I-O^{III} bond and forms a new B- O^{III} bond to take $B \equiv O$ geometry ($B_{(3)O_I}$). This

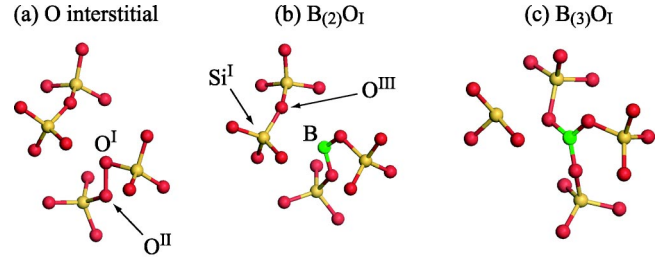


FIG. 4. (Color online) Geometric structures of total-energy minimized (a) an O interstitial, (b) $B_{(2)O_I}$, and (c) $B_{(3)O_I}$. Only a part of the atoms in a unit cell are shown to avoid visual complexity.

structural transformation results in that a dangling bond remains on Si^I . This is due to the fact that a B atom prefers the threefold coordinated geometry and that the B-O bond is stronger than the Si-O bond; this dangling bond configuration is also seen in the stable geometry of B in defect-free SiO_2 , $B_S Si_{(3)}$ [Fig. 1(a)].

D. Formation energies of various B-related defects

The results presented above clearly show that a B atom takes a variety of the stable and the metastable geometries depending on the atomic geometries around the B atom. Therefore it is important to clarify the relative stability among the stable geometries presented above. The concentrations of O vacancies and O interstitials depend on the oxygen concentration in SiO_2 . In other words, they depend on the Si concentration, i.e., the chemical potential of Si. To clarify the possible stable geometries of a B atom depending on the chemical potential of Si, we have calculated the formation energy for each geometry when the chemical potential μ_{Si} of Si, i.e., the stoichiometry of Si, is changed. The results are shown in Fig. 5. In the Si rich limit ($\mu_{Si} \approx 0$), $B_S Si_{(3)}$ geometry in which the B atom is bound to two O atoms and Si atom is stable. In the O rich limit ($\mu_{Si} \approx -8.8$, i.e., $\mu_O \approx \mu_{O(mol)}$), on the other hand, $B_{(3)O_I}$ geometry in which the B atom is threefold coordinated with

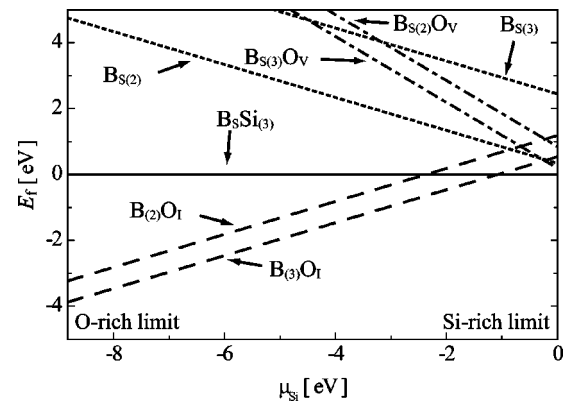


FIG. 5. The formation energy of various B-related defects for the neutral charge states as a function of the chemical potential of Si μ_{Si} . The chemical potential is measured from that of bulk Si $\mu_{Si(bulk)}$ (see text). The formation energies are measured from that of $B_S Si_{(3)}$.

nearby O atoms is stable. As seen from Fig. 5, the configuration in which a B atom binds to O vacancies is not stable in all regions of μ_{Si} due to the weakness of the Si-B bond.

To investigate the properties of a B atom in SiO_2 based on these findings, it is necessary to examine the stable geometries and the diffusion pathways of the B atom not only in defect-free SiO_2 , but also in SiO_2 with an O interstitial. The diffusion mechanisms and the activation energies of the B atom in defect-free SiO_2 have been discussed in Ref. 15. A B atom in SiO_2 with an O interstitial, however, may not diffuse similarly to that in defect-free SiO_2 due to the presence of the O interstitial. In fact, we have found that the B atom is strongly bound to the O interstitial, i.e., $\text{B}\equiv\text{O}$ structure: In an oxygen rich limit, $\mu_{\text{O}}\approx\mu_{\text{O}(\text{mol})}$, $\text{B}_{(3)}\text{O}_1$ is more stable in total energy by 4 eV than $\text{B}_\text{S}\text{O}_{(3)}$. The B atom diffuses by forming and breaking bond configurations in SiO_2 with activation energy ~ 2 eV.¹⁵ Thus the activation energy of B diffusion via the O interstitial is estimated to be more than 6 eV. This large activation energy results from breaking the strong $\text{B}\equiv\text{O}$ bonds. Consequently, this situation raises a possibility to suppress the B diffusion under oxygen rich limit. We explore the diffusion mechanism and the activation energy of the B diffusion in SiO_2 containing an O interstitial.

IV. B DIFFUSION IN SiO_2 CONTAINING O INTERSTITIAL

A. Stable geometries in charge states

In atomic diffusion in semiconductor, charge states of the defect greatly affect the diffusion mechanism and the activation energy.^{3,27,28,35,36} Thus, we first elucidate the charge dependent multi stability of a B atom in SiO_2 with an O interstitial. In the neutral charge state, we have found the stable geometry for B atom in the defect-free SiO_2 and in SiO_2 with an O interstitial [Figs. 1(b) and 4(c)]. $\text{B}_\text{S}\text{Si}_{(3)}$ and $\text{B}_{(3)}\text{O}_1$ have similar geometrical characteristics in the sense that a dangling bond remains on the Si atom. We have explored the stable geometries of the B atom with an O interstitial for charged (-1 and $+1$) states. It has been revealed that there are close analogies in the stable geometries of the B atom for each charge state between defect-free SiO_2 and SiO_2 with an O interstitial. Figure 6 shows the stable geometries. In the $+1$ charged state, the stable geometries of the B atom in the defect-free SiO_2 [Fig. 1(e) in Ref. 15] and that in SiO_2 with an O interstitial are shown in Figs. 6(a) and 6(b), respectively. Since an electron is missing on the B atom in $\text{B}_{\text{Ox}}\text{O}_{(3)}(+)$, a nonbonding orbital of O^{I} binds to one of the sp^2 orbital of the B atom, and the B atom forms the threefold coordinated geometry. In $\text{B}_{(3)}\text{O}_1(+1)$ geometry, we have found that this geometry is very similar to $\text{B}_{\text{Ox}}\text{O}_{(3)}(+)$ geometry. In other words, the B atom binds to a nonbonding orbital of O^{I} in this geometry also. In SiO_2 with an O interstitial, the B atom forms $\text{B}\equiv\text{O}$ geometry by binding to the O interstitial irrespective of its charge state being neutral or $+1$.

In -1 charged state, the stable geometry of a B atom in the defect-free SiO_2 is $\text{B}_\text{O}\text{Si}_{(5)}(-1)$ [Fig. 6(c)]. The main characteristic of this geometry is the presence of a fivefold coordinated Si^{III} that accommodates an extra electron. The B

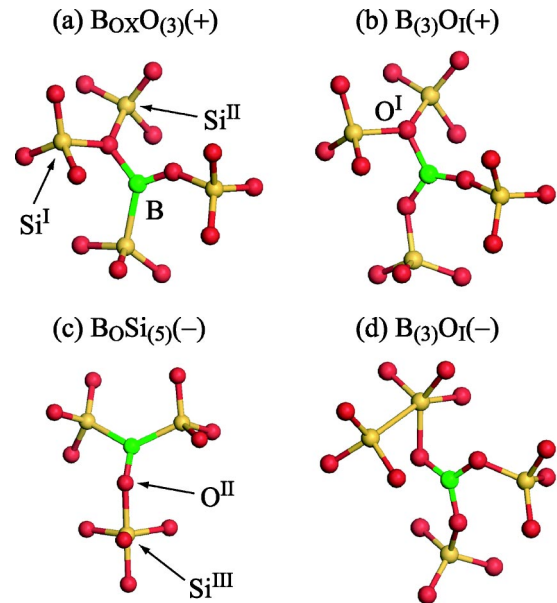


FIG. 6. (Color online) Geometric structures of total-energy minimized (a) $\text{B}_{\text{Ox}}\text{O}_{(3)}(+)$ [Fig. 1(e) in Ref. 15], (b) $\text{B}_{(3)}\text{O}_1(+)$, (c) $\text{B}_\text{O}\text{Si}_{(5)}(-)$ [Fig. 1(c) in Ref. 15], and (d) $\text{B}_{(3)}\text{O}_1(-)$. Only a part of the atoms in a unit cell are shown to avoid visual complexity.

atom forms the threefold coordinated geometry by substituting for O^{II} . The dislodged O^{II} is bound to the floating bond extended from Si^{III} . In the case of the B atom with an O interstitial, the stable geometry which is bound to the O interstitial is $\text{B}_{(3)}\text{O}_1(-1)$ [Fig. 6(d)]. This geometry can be understood as follows. In the neutral state, a dangling bond remains on Si^{I} as shown in Fig. 4(c). To accommodate an additional electron in the dangling bond, Si^{I} is bound to Si^{II} to form a Si-Si bond (floating bond). In this geometry the B atom also forms $\text{B}\equiv\text{O}$ bonds. Thus the B atom is threefold coordinated with nearby O atoms irrespective of its charge state in SiO_2 with an O interstitial.

The results presented above clearly show that the bond configurations of SiO_2 networks near a B atom are distorted depending on the B charge state. It is important to clarify the relative stability among the different charge states in their equilibria. In general, the charge state of the impurity changes depending on the chemical potential of the electron: For instance, in the case of a B atom in the defect-free SiO_2 , the positively and negatively charged state are stable, whereas the neutral state is metastable for any value of μ_e in the energy gap.¹⁵ This relative stability results in a negative-U system associated with structural transformation which takes place at the value of μ_e at the Si mid gap. Figure 7 shows the formation energies of $\text{B}_{(3)}\text{O}_1$ as a function of μ_e for the positive ($+1$; $Q=1$), neutral (0 ; $Q=0$), and negative (-1 ; $Q=-1$) charge states. As shown in Fig. 7, similar to the B atom in defect-free SiO_2 , the neutral state is the metastable geometry for any value of μ_e over the entire region of the SiO_2 energy gap. In addition, we have also found that B in SiO_2 with an O interstitial has negative-U character associated with structural transformation. The value of μ_e is in

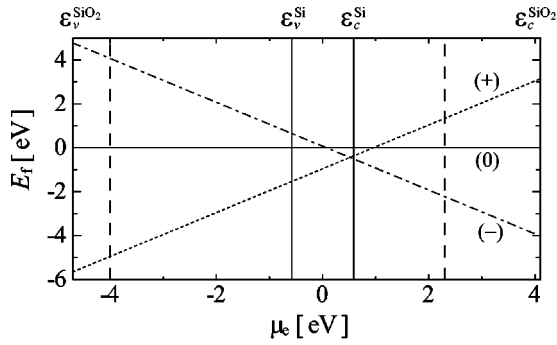


FIG. 7. The relative formation energies of $B_{(3)}O_I$ for each charge state as a function of the electron chemical potential μ_e in the energy gap of SiO_2 : The energies for the positive (+), neutral (0), and negative (-) charge states are shown. Both ends of μ are the experimental valence band top ($\epsilon_v^{SiO_2}$) and conduction band bottom ($\epsilon_c^{SiO_2}$) of SiO_2 . Those of Si (ϵ_v^{Si} and ϵ_c^{Si}) are denoted by vertical lines. The density-functional $\epsilon_v^{SiO_2}$ and $\epsilon_c^{SiO_2}$ are shown as a reference by vertical dashed lines near both ends of μ . These alignments are done by matching the theoretical and experimental thermodynamic level (Ref. 35) related to the interstitial H in SiO_2 , which is known to be located at 0.2 eV above the center of the Si gap (the energy reference here), and by using the valence-band offset of 4.3 eV between SiO_2 and Si (Refer to Ref. 37 for details).

the Si band gap, however, the positively charged state is stable except for when μ_e is located below the Si conduction band bottom.

B. Diffusion mechanism of B atoms

We have found the stable geometry of B in SiO_2 with an O interstitial for each charge state. Next, we have calculated the diffusion pathways and its activation energies. We start with the most stable geometry and explore a variety of possible diffusion pathways toward the final geometry using our constrained minimization technique. We obtained the final geometries from the corresponding starting geometry by a threefold rotation followed by a $2c/3$ nonprimitive translation. Here c is a lattice parameter of the supercell. The most favorable pathways and corresponding activation energies determined by the present calculations are shown in Fig. 8. As mentioned previously, if a B atom diffuses along the SiO_2 networks leaving an O interstitial alone, it costs more than 6 eV to break the strong B-O bond and diffuse via the SiO_2 networks. Surprisingly, as is obvious from Fig. 8, the calculated activation energies are lower than 6 eV for all the charge states. The activation energies are 2.3 eV for +1 charged state, 2.1 eV for -1 charged state, and 1.1 eV for the neutral state as shown in Fig. 8. These values are comparable to those for the diffusion of B in defect-free SiO_2 .¹⁵ This activation energy lowering can be understood as follows. Careful analyses of the diffusion process have indicated that for all the charge states, the B atom is threefold coordinated with nearby O atoms during diffusion. Thus, in oxygen rich SiO_2 , the B atom diffuses through the SiO_2 networks with an O interstitial atom by forming a ‘‘B-O complex.’’ An O atom in the B-O complex is not the same O atom in the diffusion process, but a different O atom is used

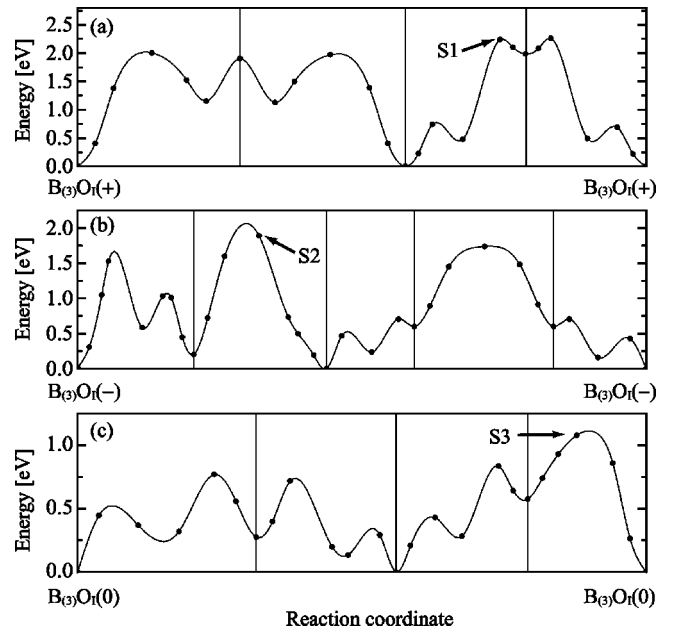


FIG. 8. Total energy variations along diffusion pathways: the $B_{(3)}O_I(+)$ \rightarrow $B_{(3)}O_I(+)$ path with positively charged (a), the $B_{(3)}O_I(-)$ \rightarrow $B_{(3)}O_I(-)$ path with negatively charged (b), and $B_{(3)}O_I(0)$ \rightarrow $B_{(3)}O_I(0)$ path with neutral (c) states. The left and right ends correspond to the initial and the final geometries. The vertical lines denote intermediate metastable geometries.

to maintain the B-O complex. One of the O atoms (O^I) in the $B\equiv O$ bonds is kicked to the next $-Si-O^{II}-Si-$ bond with a B atom and then O^{II} is kicked to the next stable site with a B atom. During this process, the B atom can diffuse by keeping the $B\equiv O$ bonds without forming the Si-B bond. Once the B atom formed the Si-B bond, the activation energy for the B diffusion should be higher than this diffusion mechanism due to the fact that the B-O bond is much stronger than the Si-B bond. In the present diffusion processes, however, Si-B bonds are not formed. Thus the activation energies are remarkably suppressed. Consequently we have found that in an equilibrium condition the B atom diffuses in SiO_2 with activation energies of 2.1–2.3 eV irrespective of the presence or absence of an O interstitial.

Variation of atomic geometries and bond configurations during the diffusion are extremely interesting and further clarify the specific characteristics of the charge states. Figure 9 shows the geometries near the saddle points S1, S2, and S3 shown in Fig. 8. In the saddle-point geometry of S1 [Fig. 9(a)] for the +1 charged state, a nonbonding orbital of the O atom is bound to the sp^2 -hybridized orbital of the B atom. In other geometries on the diffusion pathways, the sp^2 -hybridized orbital of the B atom always binds to the nonbonding orbital of the O atom, and diffuses via the SiO_2 networks with the O interstitial. In the saddle-point geometry of S2 [Fig. 9(b)] for the -1 charged state, many floating bonds are formed to accommodate an additional electron. In the -1 charged state, an additional electron is continuously accommodated in the floating bond, and the B atom diffuses by forming and breaking that bond with the O interstitial. In the neutral state, the saddle-point geometry is S3 [Fig. 9(c)].

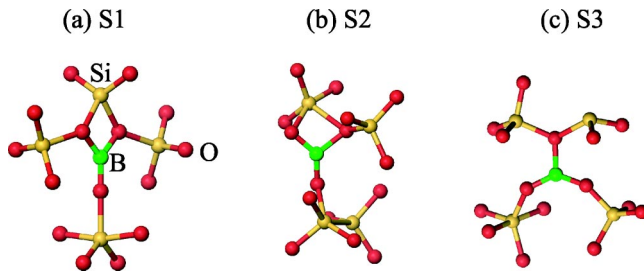


FIG. 9. (Color online) Saddle-point geometries during the B diffusion for the +1 charged state (a), the -1 charged state (b), and the neutral state. Only a part of atoms in a unit cell are shown to avoid visual complexity.

As seen from the figure, there is a dangling bond on the Si atom. Furthermore the dangling bond is also present on the Si atom during diffusion. It has been found that the B-O complex diffuses via the SiO₂ networks accompanied with the dangling bond on Si.

V. SUMMARY

We have presented first-principle calculations that clarify the stable geometries and the diffusion mechanisms of a B atom in defect-free SiO₂ and SiO₂ with point defects. We have found that the B atom takes various stable and metastable geometries in SiO₂, depending on its charge state and the local network around the B atom. In the case of a B atom in defect-free SiO₂, B_SSi₍₃₎ geometry becomes stable for the neutral state and metastable for +1 and -1 charged states. The structural transformation between the charge states can be systematically understood by considering the wave function distribution and its occupation. In the neutral state the B atom is threefold coordinated with a nearby O atom, whereas a dangling bond remains on the Si atom. This is because the B-O bond is stronger than the Si-O bond. In the -1 charged state, to accommodate an additional electron, the Si atom forms a floating bond with the nearby Si atom associated

with large structural deformation. In the +1 charged state, due to the absence of an electron, the Si atom forms an sp^2 -like bond configuration to decrease the p -component in the occupied states. These are the common characteristics of the stable geometries between defect-free SiO₂ and SiO₂ with an O interstitial at each charge state.

Under Si rich conditions, the B_SSi₍₃₎ geometry is the most stable, whereas under O rich conditions, the B₍₃₎O₁ geometry is most stable. We have also found that the B atom in SiO₂ with an O vacancy is energetically unstable in all regions of μ_{Si} due to the weakness of the Si-B bond. In the case of a B atom in SiO₂ with an O interstitial, the B atom forms the B-O complex with an O atom irrespective of its charge states. Unexpectedly once the B atom forms the B-O complex, the B atom diffuses via SiO₂ networks with an O interstitial by breaking and forming bond configurations. We have found that the activation energies of the B-O complex are 2.1–2.3 eV. Since the activation energies of the B atom in defect-free SiO₂ were found to be 2.2–2.3 eV,¹⁵ the activation energies of the B atom are 2.1–2.3 eV irrespective of the presence or absence of the O interstitial. These values agree well with those obtained experimentally.¹²

ACKNOWLEDGMENTS

One of us (M.O.) would like to acknowledge helpful discussions with Dr. T. Akiyama, Dr. H. Kageshima, and Dr. M. Uematsu. Computations were done at the Science Information Processing Center, University of Tsukuba, and at the Research Center of Computational Science, Okazaki National Institute. This work was partly supported by Grant-in-Aid for Scientific Research Nos. 14550020 and 14550021 of the Ministry of Education, Science and Culture of Japan, by ACT-JST (Japan Science and Technology Corporation), and by a program for the “Promotion of Leading Researches” in Special Coordination Funds for Promoting Science and Technology by the Ministry of Education, Culture, Sports, Science and Technology.

*Present address: Institute for Solid State Physics, University of Tokyo, Kashiwanoha 5-1-5, Kashiwa, Chiba 277-8581, Japan.

¹W. Frank, U. Gösele, H. Mehrer, and A. Seeger, in *Diffusion in Crystalline Solids*, edited by G.E. Murch and A.S. Nowick (Academic, New York, 1984).

²P.M. Fahey, P.B. Griffin, and J.D. Plummer, *Rev. Mod. Phys.* **61**, 289 (1989).

³R. Car, P.J. Kelly, A. Oshiyama, and S.T. Pantelides, *Phys. Rev. Lett.* **52**, 1814 (1984); **54**, 360 (1985).

⁴C.S. Nichols, C.G. Van de Walle, and S.T. Pantelides, *Phys. Rev. Lett.* **62**, 1049 (1989); *Phys. Rev. B* **40**, 5484 (1989).

⁵K.C. Pandey, *Phys. Rev. Lett.* **57**, 2287 (1986); K.C. Pandey and E. Kaxiras, *ibid.* **66**, 915 (1991).

⁶P.E. Blöchl, E. Smargiassi, R. Car, D.B. Laks, W. Andreoni, and S.T. Pantelides, *Phys. Rev. Lett.* **70**, 2435 (1993).

⁷H. Bracht, E.E. Haller, and R. Clark-Phelps, *Phys. Rev. Lett.* **81**, 393 (1998).

⁸A. Ural, P.B. Griffin, and J.D. Plummer, *Phys. Rev. Lett.* **83**, 3454 (1999).

⁹J.R. Pfister, F.K. Baker, T.C. Mele, H-H Tseng, P.J. Tobin, J.D. Hayden, J.W. Miller, C.D. Gunderson, and L.C. Parrillo, *IEEE Trans. Electron Devices* **37**, 1842 (1990). Successful fabrication of 1.3-nm gate oxides is recently reported: G. Timp *et al.*, in *IDEM Technical Digest* (IEEE, Piscataway, NJ, 1997), p. 930; T. Sorsch *et al.*, in *Proceedings of the Symposium on VLSI Technology, Digest of Technical Papers* (IEEE, Piscataway, NJ, 1998), p. 222.

¹⁰C.Y. Chang, C-Y Lin, J.W. Chou, C.C-H Hsu, H-T Pan, and J. Ko, *IEEE Electron Device Lett.* **15**, 437 (1994).

¹¹J.J. Sung and C.Y. Lu, *IEEE Trans. Electron Devices* **37**, 2312 (1990).

¹²T. Aoyama, H. Tashiro, and K. Suzuki, *J. Electrochem. Soc.* **146**, 1879 (1999), and references therein.

¹³R.B. Fair, *IEEE Electron Device Lett.* **17**, 242 (1996); **144**, 708 (1997).

¹⁴W.B. Fowler and A.H. Edwards, *J. Non-Cryst. Solids* **222**, 33 (1997).

¹⁵M. Otani, K. Shiraishi, and A. Oshiyama, *Phys. Rev. Lett.* **90**,

- 075901 (2003).
- ¹⁶H. Nishikawa, R. Tohmon, Y. Ohki, K. Nagasawa, and Y. Hama, *J. Appl. Phys.* **65**, 4672 (1989).
- ¹⁷J.P. Perdew, K. Burke, and M. Ernzerhof, *Phys. Rev. Lett.* **77**, 3865 (1996); J.P. Perdew, K. Burke, and Y. Wang, *Phys. Rev. B* **54**, 16 533 (1996).
- ¹⁸Codes used in the present work are based on Tokyo Ab initio Program Package (TAPP) developed by us: J. Yamauchi, M. Tsukada, S. Watanabe, and O. Sugino, *Phys. Rev. B* **54**, 5586 (1996); H. Kageshima and K. Shiraishi, *ibid.* **56**, 14 985 (1997); O. Sugino and A. Oshiyama, *Phys. Rev. Lett.* **68**, 1858 (1992).
- ¹⁹The inclusion of spin degree of freedom is important: The total energy gain due to spin-polarization is typically 0.2–0.5 eV, and the spin splittings of Kohn-Sham levels are 1.5–2.0 eV.
- ²⁰N. Troullier and J.L. Martins, *Phys. Rev. B* **43**, 1993 (1991).
- ²¹D. Vanderbilt, *Phys. Rev. B* **41**, 7892 (1990).
- ²²The convergence of the calculational parameters are examined by using the cutoff energies of 25, 49, and 64 Ry, and the Γ point and the eight k point samplings in BZ. The calculated total energy differences are found to converge within 0.02 eV.
- ²³S. Jeong and A. Oshiyama, *Phys. Rev. Lett.* **81**, 5366 (1998).
- ²⁴S.T. Pantelides, *Phys. Rev. Lett.* **57**, 2979 (1986).
- ²⁵D.C. Allan and M.P. Teter, *J. Am. Ceram. Soc.* **73**, 3247 (1990).
- ²⁶K.C. Snyder and W.B. Fowler, *Phys. Rev. B* **48**, 13 238 (1993).
- ²⁷M. Boero, A. Pasquarello, J. Sarnthein, and R. Car, *Phys. Rev. Lett.* **78**, 887 (1997).
- ²⁸A. Oshiyama, *Jpn. J. Appl. Phys.* **37**, L232 (1998).
- ²⁹P.E. Blöchl, *Phys. Rev. B* **62**, 6158 (2000).
- ³⁰*CRC Handbook of Chemistry and Physics*, edited by D.R. Lide, 81st ed. (CRC Press, Florida, 2000).
- ³¹G. Pacchioni and G. Ierano, *Phys. Rev. B* **56**, 7304 (1997).
- ³²K.-O. Ng and D. Vanderbilt, *Phys. Rev. B* **59**, 10 132 (1999).
- ³³D.R. Hamann, *Phys. Rev. Lett.* **81**, 3447 (1998).
- ³⁴Y.-G. Jin and K.J. Chang, *Phys. Rev. Lett.* **86**, 1793 (2001).
- ³⁵S. Jeong and A. Oshiyama, *Phys. Rev. Lett.* **86**, 3574 (2001).
- ³⁶J.W. Jeong and A. Oshiyama, *Phys. Rev. B* **64**, 235204 (2001).
- ³⁷P.E. Blöchl and J.H. Stathis, *Phys. Rev. Lett.* **83**, 372 (1999).